Am J Physiol Cell Physiol 315: C885–C896, 2018.
First published November 7, 2018; doi:10.1152/ajpcell.00120.2018.

RESEARCH ARTICLE

Adipose-derived mesenchymal stem cells accelerate diabetic wound healing in a similar fashion as bone marrow-derived cells

Jianming Guo,[1,2,5]* Haidi Hu,[2,3,5]* Jolanta Gorecka,[2,5] Hualong Bai,[2,5] Hao He,[2,5] Roland Assi,[2,5] Toshihiko Isaji,[2,5] Tun Wang,[2,5] Ocean Setia,[2,5] Lara Lopes,[2,5] Yongquan Gu,[1] and Alan Dardik[2,4,5]

[1]*Department of Vascular Surgery, Xuanwu Hospital, Capital Medical University and Institute of Vascular Surgery, Capital Medical University, Beijing, China;* [2]*Department of Surgery, Yale School of Medicine, New Haven, Connecticut;* [3]*Department of Surgery, the First Hospital, China Medical University, Shenyang, China;* [4]*Department of Surgery, VA Connecticut Healthcare System, West Haven, Connecticut; and* [5]*Vascular Biology and Therapeutics Program, Yale School of Medicine, New Haven, Connecticut*

Submitted 29 March 2018; accepted in final form 6 November 2018

Guo J, Hu H, Gorecka J, Bai H, He H, Assi R, Isaji T, Wang T, Setia O, Lopes L, Gu Y, Dardik A. Adipose-derived mesenchymal stem cells accelerate diabetic wound healing in a similar fashion as bone marrow-derived cells. *Am J Physiol Cell Physiol* 315: C885–C896, 2018. First published November 7, 2018; doi: 10.1152/ajpcell.00120.2018.—We have previously shown that bone marrow-derived mesenchymal stem cells (BMSC) accelerate wound healing in a diabetic mouse model. In this study, we hypothesized that adipose tissue-derived stem cells (ADSC), cells of greater translational potential to human therapy, improve diabetic wound healing to a similar extent as BMSC. In vitro, the characterization and function of murine ADSC and BMSC as well as human diabetic and nondiabetic ADSC were evaluated by flow cytometry, cell viability, and VEGF expression. In vivo, biomimetic collagen scaffolds containing murine ADSC or BMSC were used to treat splinted full-thickness excisional back wounds on diabetic C57BL/6 mice, and human healthy and diabetic ADSC were used to treat back wounds on nude mice. Wound healing was evaluated by wound area, local VEGF-A expression, and count of CD31-positive cells. Delivery of murine ADSC or BMSC accelerated wound healing in diabetic mice to a similar extent, compared with acellular controls ($P < 0.0001$). Histological analysis showed similarly increased cellular proliferation ($P < 0.0001$), VEGF-A expression ($P = 0.0002$), endothelial cell density ($P < 0.0001$), numbers of macrophages ($P < 0.0001$), and smooth muscle cells ($P < 0.0001$) with ADSC and BMSC treatment, compared with controls. Cell survival and migration of ADSC and BMSC within the scaffolds were similar ($P = 0.781$). Notch signaling was upregulated to a similar degree by both ADSC and BMSC. Diabetic and nondiabetic human ADSC expressed similar levels of VEGF-A ($P = 0.836$) in vitro, as well as in scaffolds ($P = 1.000$). Delivery of human diabetic and nondiabetic ADSC enhanced wound healing to a similar extent in a nude mouse wound model. Murine ADSC and BMSC delivered in a biomimetic-collagen scaffold are equivalent at enhancing diabetic wound healing. Human diabetic ADSC are not inferior to nondiabetic ADSC at accelerating wound healing in a nude mouse model. This data suggests that ADSC are a reasonable choice to evaluate for translational therapy in the treatment of human diabetic wounds.

adipose; diabetes; mesenchymal stem cells; tissue scaffolds; wound healing

INTRODUCTION

Diabetic foot ulcers (DFU) are a major complication of diabetes mellitus that frequently lead to amputation or even death (15, 17). The incidence of DFU is increasing owing to the worldwide increasing prevalence of diabetes and the prolonged life expectancy of diabetic patients; DFU impose a considerable morbidity and mortality along with substantial social, medical, and economic burdens. Thus, developing new and efficient treatment strategies for improving DFU healing is urgently needed (15, 21, 31).

The underlying mechanism of DFU development is complicated and involves a multifactorial etiology including hypoxia, dysfunctional fibroblasts and epidermal cells, impaired angiogenesis and neovascularization, high levels of metalloproteases, damage secondary to reactive oxygen species, and advanced glycation end products, as well as decreased host immune resistance and neuropathy (16). Most currently available approaches for diabetic wound healing have only limited therapeutic efficacy (3, 22). In recent years, a mesenchymal stem cell-based therapeutic approach targeting improved neovascularization and cutaneous regeneration has demonstrated efficacy in wound healing, providing a potentially comprehensive solution by addressing multiple etiologic factors (29). We have previously shown that bone marrow-derived mesenchymal stem cells (BMSC) accelerate wound healing in a diabetic mouse model (2).

Although BMSC are readily available in animal models, adipose tissue-derived stem cells (ADSC) carry several advantages including ease of extraction without invasive procedures, increased abundance, and possibility for rapid expansion (8). Additionally, ADSC appear to be less immunogenic and more genetically stable in long-term culture compared with BMSC (14, 23).

We hypothesized that ADSC have a similar therapeutic effect in improving DFU healing as BMSC. We tested this hypothesis in a diabetic C57BL/6 mouse full-thickness splinted back wound model. We subsequently compared the efficacy of

* J. Guo and H. Hu contributed equally to this work.

Address for reprint requests and other correspondence: A. Dardik, Yale University School of Medicine, 10 Amistad Street, Room 437, PO Box 208089, New Haven, CT 06520-8089 (e-mail: alan.dardik@yale.edu).

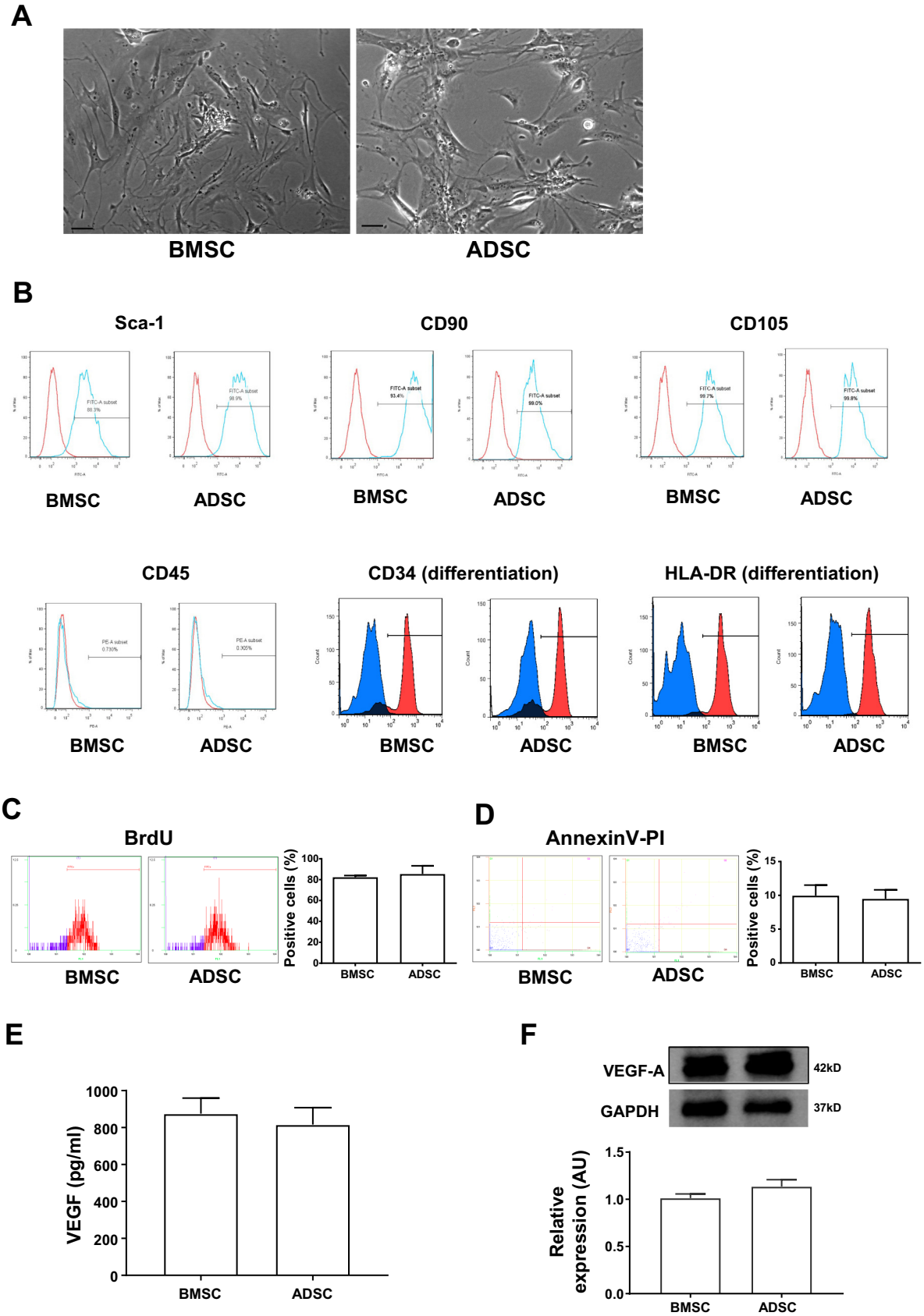

human diabetic and nondiabetic ADSC in a similar wound model in nude mice.

MATERIALS AND METHODS

Animals. All animal studies were performed in strict compliance with federal guidelines and approved by Yale University's Institutional Animal Care and Use Committee. Male C57BL/6 mice (8–12 wk; 20–30 g; Jackson Laboratory) were used for induction of diabetes before creating full-thickness back wounds. Mice were injected daily for 7 days with streptozotocin (50 mg/kg IP; Tocris Biosciences, Bristol, UK). After ~1 wk hyperglycemia was confirmed with a glucometer; only mice with blood glucose levels greater than 300 mg/dl were used. For experiments with human ADSC, nude mice (20 mice, 8–12 wk; 20–30 g; Jackson Laboratory) were used in a similar fashion.

Mice were anesthetized with ketamine (100 mg/kg) and xylazine (10 mg/kg). Back hair was removed using a chemical depilatory (Nair). A full-thickness skin wound (5 mm diameter) was created on the back, and a silicone ring (10 mm inner diameter, 0.5 mm thick) was sutured into place surrounding the wound to prevent healing by contracture (12). Collagen scaffolds (see below) were then unfolded and placed onto the wound surface. Wound size measurements were obtained every other day postoperatively. Mice were briefly anesthetized with isoflurane and wounds were photographed with an Olympus SP-800 UZ camera mounted on a tripod at a fixed distance; a ruler was included in the digital photo for scale. Wound areas were analyzed using ImageJ software (National Institutes of Health, Bethesda, MD). At the completion of the study, mice were euthanized and the wounds with surrounding tissues were harvested and placed in 10% phosphate-buffered formalin overnight. Afterwards, the samples were paraffin embedded and stained for histochemical analysis as described below.

MSC isolation and expansion. Murine bone marrow-derived MSC or adipose-derived MSC were obtained from C57BL/6 mice femoral bone marrow or abdominal fat as previously reported (1, 2). MSC were cultured in EGM-2 media (Lonza, Basel, Switzerland), consisting of 10% FBS (GIBCO) and 1% penicillin-streptomycin (GIBCO), 2 mM L-glutamine (Corning Life Sciences) in plastic dishes at 37°C in 5% humidified CO_2. They were continuously cultured for further use, and cell *passages 2–6* were used in this study.

MSC identity was confirmed by FACS analysis of *passage 2* cells as previously described (2). MSC were identified using anti-CD34, anti-CD90, anti-Sca-1, anti-CD105, anti-CD45, anti-HLA-DR (BioLegend), using an LSRII flow cytometer (BD Biosciences).

Green fluorescence dye DiOC18(3),3,3′ was used to label some of the cells before their addition to the collagen gel (see below). DiOC18(3)-positive cells were detected by immunofluorescence on frozen sections taken on *postoperative day 5*. MSC cell proliferation was detected using BrdU labeling. In brief, cell culture medium was removed, and the BrdU labeling solution (10 μM) was added to the cell culture dish. The cells were then incubated at 37°C for 2 h. PBS was used to wash cells twice after removal of the labeling solution. The cells were then fixed with 4% formaldehyde (15 min., room temperature). The cells were then incubated in antibody staining buffer (1 ml) with FITC-conjugated anti-BrdU primary antibody overnight at room temperature. The samples were then washed with Triton X-100 permeabilization buffer three times. Flow cytometry was then used to detect the expression levels of BrdU.

Apoptosis was evaluated using an AnnexinV-FITC/propidium iodide (PI) kit; approximately 1×10^5 cells were harvested and washed twice with PBS. AnnexinV-FITC binding buffer (195 μl) was added to the resuspended cells, followed by a 30 min incubation in 5 μl AnnexinV-FITC at 37°C in the dark. Cells were then centrifuged at 1,000 *g* for 5 min, and 190 μl binding buffer with 10 μl PI was added. Flow cytometry was then used to count the number of apoptotic cells.

Collagen scaffolds. Collagen scaffolds were constructed by adding type 1 rat tail collagen (3 ml of 5% solution; Enzo Life Sciences) to PBS (1 ml) and 10× DMEM (0.5 ml; Sigma-Aldrich). pH was then adjusted to 7.0 using drop wise addition of 1 M NaOH or 0.1 M NaOH, as previously described (2). For cellular constructs, 2×10^6 MSC in 0.5 ml solution were added to the collagen gel; for acellular constructs, an equal volume of PBS was used (final volume 5 ml). The collagen solution was allowed to solidify within a rectangular mold (room temperature, 30 min) and was then compressed between glass plates (5 min). The compressed collagen sheet was then rolled tightly and incubated in tissue culture medium (37°C, 72 h). After 72 h, collagen roll was unfolded for in vivo application.

Immunohistochemistry and immunofluorescence. Immunohistochemistry and immunofluorescence were performed as previously described (2).The primary antibodies used in our experiment included anti-VEGF-A (rabbit: 1:100; Santa Cruz Biotechnology), Ki67 (rabbit: 1:200; Abcam), anti-caspase 3 (rabbit: 1:1,000; Cell Signaling), F4/80 (rat: 1:100; Abcam), α-smooth muscle actin (rabbit: 1:100; Abcam), vimentin (rabbit: 1:500; Abcam). For immunohistochemistry, after developing with diaminobenzidine and counterstaining with hematoxylin, photomicrographs were obtained and positive cells were manually counted and reported as a percentage of total cells. Cells were considered positive if they stained for both diaminobenzidine (brown) and hematoxylin (purple), indicating signal of interest and nuclei, respectively. Four sections per slide were counted at random per sample and the average number of cells of the total number of cells was recorded.

For immunofluorescence, after incubation with primary antibodies overnight, the sections were incubated with secondary antibodies at room temperature for 1 h using goat anti-rabbit Alexa Fluor 488 (Life Technologies, Grand Island, NY), donkey anti-goat Alexa-Fluor-488 (Life Technologies), or donkey anti-rabbit Alexa-Fluor-568 (Life Technologies). Sections were stained with SlowFade Gold Antifade Mountant with DAPI (Life Technologies) and a coverslip was applied. Digital fluorescence images were captured after optimal exposure time was determined based on control samples to exclude background staining. The intensity of the immunoreactive signal was measured using ImageJ software, and the signal intensity was measured after subtraction of the background signal. To determine number of positive cells, four sections were chosen at random and cells stained with DAPI and signal of interest were counted and averaged.

Human ADSC cell culture. Human nondiabetic and diabetic ADSC were obtained from Lonza. Cells from one healthy and one diabetic patient were used in this study. ADSC *passages 3–4* were cultured and maintained in ADSC basal medium with addition of the ADSC-GM SQ Kit (Lonza). ADSC from *passage 2* were cultured for 24 h to reach nearly 90% confluence. Prior to use, the medium was changed to FBS-free medium for 12 h.

Western blotting. ADSC were washed twice with cold PBS, and cell lysates were extracted with RiPA Lysis buffer (Millipore). Equal amounts of protein (20–40 μg) were separated on a 10% SDS-PAGE gel and electrophoretically transferred onto polyvinylidene difluoride

Fig. 1. Similar characterization of murine adipose tissue-derived stem cells (ADSC) and bone marrow-derived mesenchymal stem cells (BMSC) in vitro. *A*: photomicrographs show morphology of BMSC (*left*) and ADSC (*right*), immediately after isolation (×200, scale bar = 50 μm). *B*: FACS analysis confirms identity of murine BMSC and ADSC with positive expression of Sca-1, CD90, CD105 and lack of expression of CD45, CD34, and HLA-DR. *C*: FACS confirms similar proliferation (BrdU) of murine BMSC and ADSC. *D*: FACS confirms similar apoptosis (AnnexinV-PI) of murine BMSC and ADSC. *E*: VEGF expression by BMSC and ADSC quantified by ELISA ($P > 0.05$, $n = 3$). *F*: quantification of VEGF-A expression in BMSC and ADSC by Western blotting. Histogram depicts relative expression in both groups ($P = 0.0654$, $n = 3$ for each in vitro experiment).

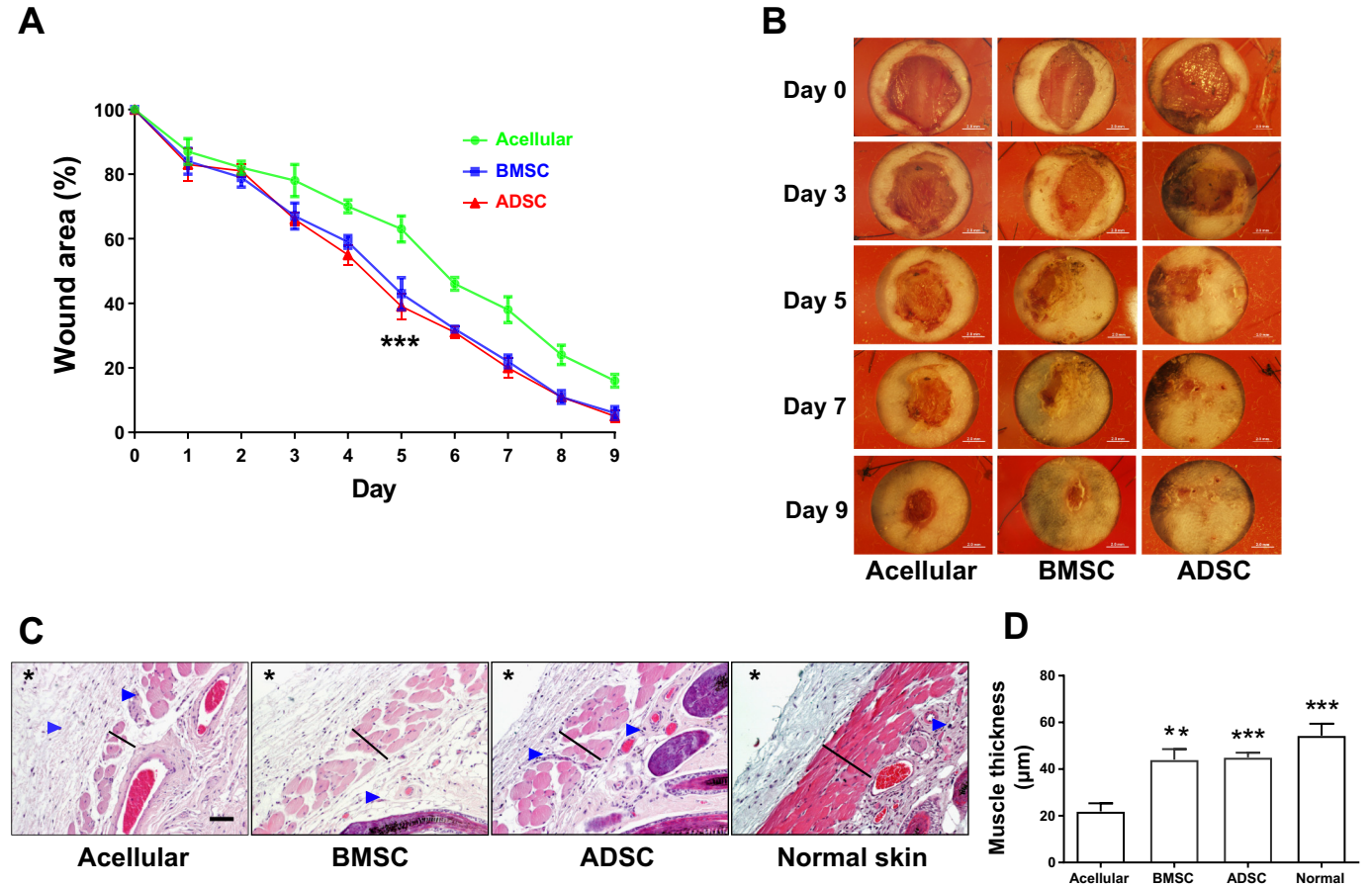

Fig. 2. Murine bone marrow-derived mesenchymal stem cells (BMSC) and adipose tissue-derived stem cells (ADSC) show equivalent wound healing in vivo. *A*: line graph shows wound size over time (***$P < 0.001$, two-way ANOVA, $n = 5$ for each group). *B*: representative images of wounds at *days 0*, *3*, *5*, *7*, and 9 (scale bar: 2 mm). *C*: hematoxylin-eosin stain of wound tissue. *Left* to *right*: acellular, BMSC, ADSC, and normal skin at *day 5* (×200, scale bar = 100 μm). Black line represents muscle thickness, black star in *top left* corner is oriented to skin surface; and arrowheads point to inflammatory cell foci above and below the muscle layer. *D*: quantification of muscle thickness by bar graph (**$P < 0.01$, ***$P < 0.001$, $n = 3$ for each group).

microporous membranes (0.45 μm pore size, Immobilon, Millipore). Membranes were then blocked in TBS with Tween 20 (TBS-T) containing 5% bovine serum albumin for 1 h at room temperature and incubated in anti-VEGF-A (1:500; Abcam 51745) or GAPDH (1: 3,000, Cell Signaling) primary antibodies overnight at 4°C on a shaker. After membranes were washed with TBS-T and incubated with either anti-rabbit or anti-mouse horseradish peroxidase-conjugated secondary antibody (Cell Signaling) for 1 h at room temperature, immunocomplexes were visualized using chemiluminescence (GE) following the manufacturer's protocol.

ELISA assay. Collagen scaffolds were prepared as previously described. The scaffolds were then incubated at 37°C for 72 h. The medium was subsequently collected and VEGF concentration was determined using mouse Quantikine ELISA kit according to manufacturer's instructions (R&D Systems). Briefly, samples, buffers, and standards were prepared according to packaging instructions, and 50 μl of Assay Diluent was added to each well of a previously antibody-coated 96-well plate. Two hundred microliters of standard, control, or scaffold sample were then added in duplicate pairs to consecutive wells, followed by a 2 h incubation at room temperature. Each well was then washed three times with washing buffer. VEGF conjugate (200 μl) was then added to each well, followed by a 2 h incubation at room temperature. Finally, 200 μl of substrate solution were added to each well and after a 20 min incubation at room temperature, stop buffer was added. Concentrations were then determined using a microplate reader at 450 nm.

Statistical analyses. Data are expressed as means ± SD. Statistical analysis was performed using an independent Student's *t*-test for two groups of data and analysis of variance (ANOVA) followed by Scheffé's post hoc test for multiple comparisons. Statistical analysis was performed by an independent statistician using SPSS statistic software (version 15.0; SPSS, Chicago, IL) and GraphPad Prism software (version 5.0; La Jolla, CA). $P < 0.05$ was considered significant.

RESULTS

Similar characterization of murine ADSC and BMSC in vitro. We have previously shown that delivery of activated murine BMSC in a collagen scaffold enhances wound healing

Fig. 3. Murine bone marrow-derived mesenchymal stem cells (BMSC) and adipose tissue-derived stem cells (ADSC) show equivalent effects on cell infiltration into wounds in vivo. *A*: representative images and bar graph showing mesenchymal stem cells (MSC) labeled with DiOC18(3) in vitro and in vivo. *Left*: in DMEM medium in vitro; *middle*: MSC labeled in the scaffold culture after 72 h in vitro; *right*: labeled cells in vivo at *day 5* ($n = 3$, ×200, scale bar = 50 μm). *B*: representative images of immunohistochemistry for α-actin, CD31, F4/80, Ki67, caspase-3, and VEGF-A ($n = 4$ for each group, ×400, scale bar = 50 μm). *C* and *D*: quantification of percentage of positive cells (***$P < 0.001$, $n = 4$).

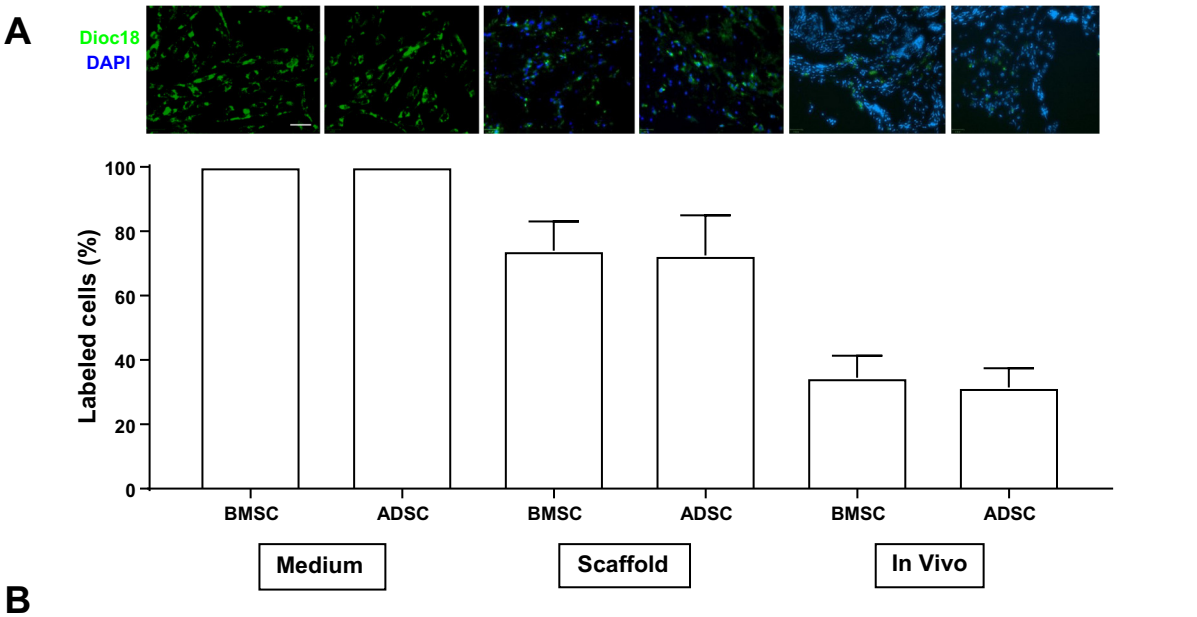

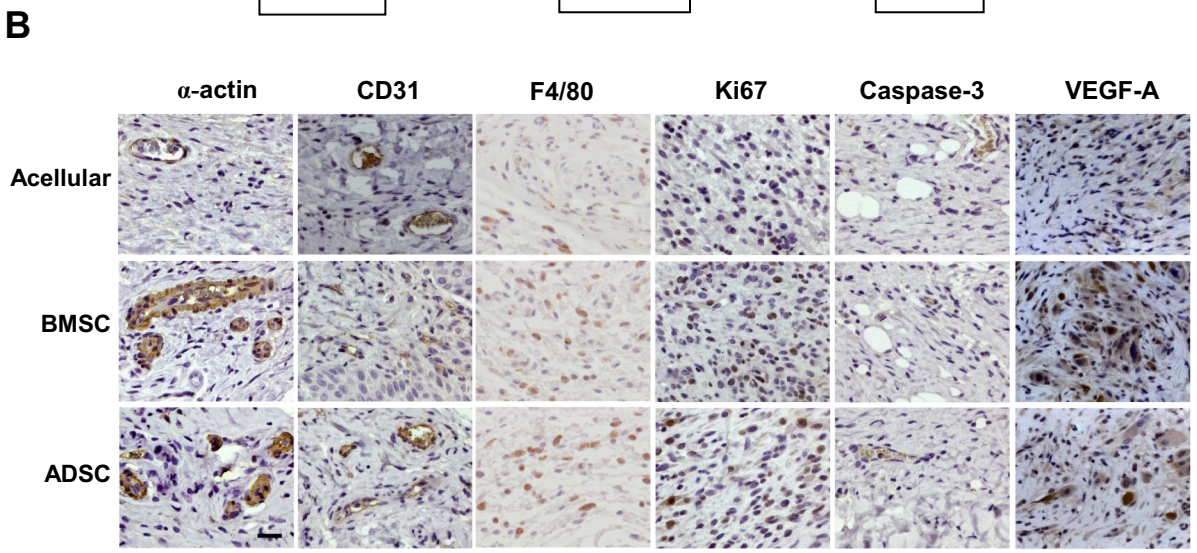

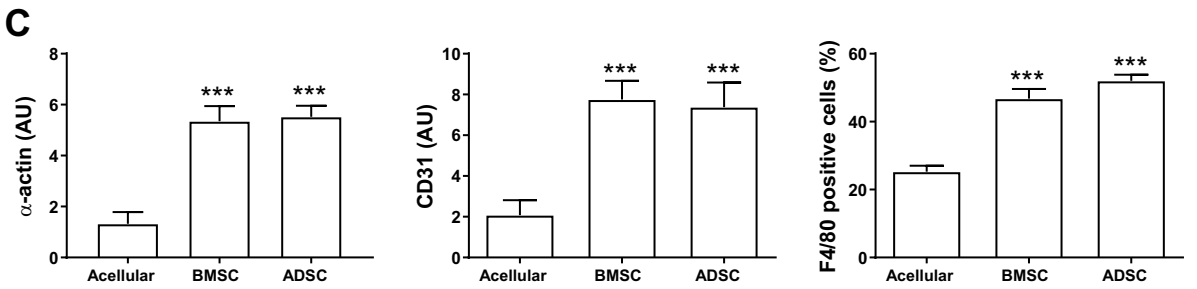

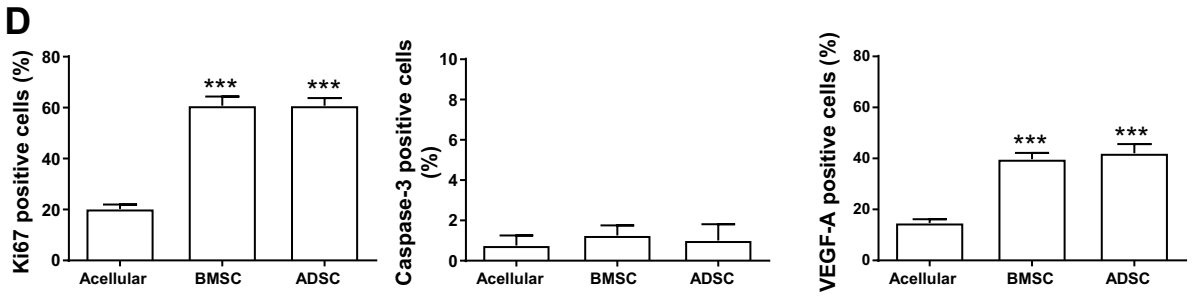

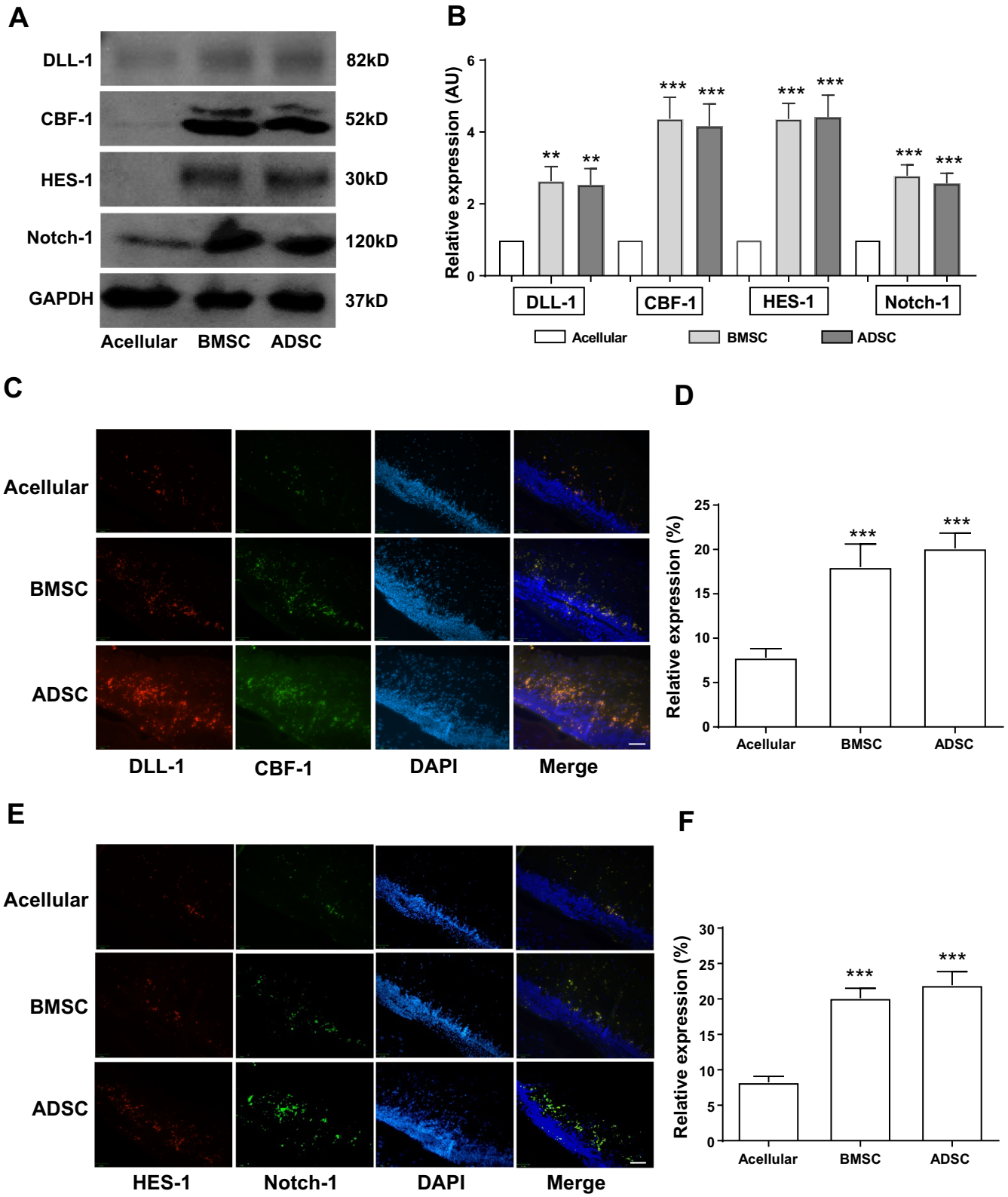

Fig. 4. Murine bone marrow-derived mesenchymal stem cells (BMSC) and adipose tissue-derived stem cells (ADSC) show equivalent effects on Notch expression in vivo. *A*: Western blot of Notch signaling pathway proteins. *B*: quantification of relative protein expression in scaffolds with BMSC or ADSC compared with acellular scaffolds (**$P < 0.01$, ***$P < 0.001$). *C*: immunofluorescence for DLL-1 and CBF-1 in a scaffold with BMSC or ADSC and acellular scaffold, *day 7* (×200, scale bar = 50 μm). *D*: quantification of DLL-1 and CBF-1 immunofluorescence colocalization (***$P < 0.001$, $n = 3$ for each group). *E*: immunofluorescence for *HES-1* and Notch-1 in a scaffold with BMSC or ADSC and acellular scaffold, *day 7* (×200, scale bar = 50 μm). *F*: quantification of *HES-1* and Notch-1 immunofluorescence colocalization (***$P < 0.001$, $n = 3$ for each group).

in a diabetic mouse model (2). To improve the translational application of this model, we determined whether ADSC have similar efficacy to BMSC in several assays. Both BMSC and ADSC showed similar morphology in vitro (Fig. 1*A*), as well as expression of surface markers consistent with mesenchymal stem cell identity (Fig. 1*B*) (9). We used CD34 and HLA-DR surface markers to show the different phenotype of undifferentiated versus differentiated cells. CD34 expression in undifferentiated BMSC and ADSC was 0.31% and 0.24%, respectively, and increased to 84.5% and 82.1%, respectively, in differentiated cells (Fig. 1*B*). Similarly, HLA-DR expression increased from 0.09% and 0.05% to 98.86% and 92.42% in BMSC and ADSC cells, respectively, after differentiation (Fig. 1*B*). Both cell lines also expressed similar rates of proliferation and apoptosis in vitro (Fig. 1, *C* and *D*). There was no difference in the amount of VEGF secreted between the two cell lines, as measured by ELISA and Western blotting (VEGF-A detected by Western blotting) (Fig. 1, *E* and *F*).

Murine BMSC and ADSC show equivalent acceleration of wound healing in vivo. As expected, diabetic C57BL/6 mice had increased blood glucose levels (392.0 ± 25.4 mg/dl vs. 132.4 ± 20.4 mg/dl, *day 7*; $P < 0.0001$; $n = 4$) and reduced body weight (19.7 ± 1.2 g vs. 23.0 ± 1.5 g, *day 28*; $P = 0.0019$; $n = 4$) compared with control mice. We have previously shown that scaffolds containing BMSC significantly improve the rate of wound healing in splinted back wounds, compared with acellular controls (2). Wounds treated with ADSC accelerated healing to the same degree as BMSC (ADSC, 39 ± 3% vs. BMSC, 43 ± 5%; $P = 0.304$, post hoc), both improved compared with acellular scaffolds (63 ± 4%; $P < 0.0001$, ANOVA; Fig. 2, *A* and *B*).

Wound histology showed a significant increase in muscle thickness and less inflammatory cell infiltration in both ADSC- and BMSC-treated wounds, as compared with acellular controls ($P < 0.0001$); there was no significant difference in the average muscle thickness in wounds treated with scaffolds containing BMSC or ADSC ($P = 0.989$, post hoc; Fig. 2, *C* and *D*).

We next determined whether BMSC and ADSC treatment results in attraction of similar numbers of infiltrating cells into the wound environment to accelerate healing. BMSC and ADSC were labeled with the cell tracking dye DiOC18(3) before incorporation into collagen scaffolds. Both immediately after labeling as well as after 3 days in vitro, cells in both treatment conditions showed similar rates of dye labeling. After 5 days in vivo, there were similar numbers of cells infiltrating into scaffolds containing BMSC or ADSC ($P = 0.781$; Fig. 3*A*). Further, we transfected some BMSC and ADSC with a lentivirus carrying green fluorescence protein (GFP) before incorporation in scaffold, and harvested them from mouse back wounds at *day 5*. Analysis revealed similar expression of GFP-containing cells in both BMSC and ADSC wounds (data not shown).

There were increased numbers of α-actin-positive cells in MSC-treated wounds, compared with acellular scaffolds ($P < 0.0001$, post hoc), while the number of α-actin-positive cells in wounds treated with ADSC and BMSC was similar ($P = 0.786$, post hoc) (Fig. 3, *B* and *C*). Similarly, there was increased expression of CD31-positive cells in MSC-treated wounds compared with acellular scaffolds, and similar numbers of positive cells in wounds treated with ADSC or BMSC ($P = 0.409$, post hoc) (Fig. 3, *B* and *C*). In addition, there were also more F4/80-positive cells in wounds treated with scaffolds containing BMSC or ADSC compared with wounds treated with acellular scaffolds ($P < 0.0001$). There were more Ki67-positive cells in both BMSC- and ADSC-containing scaffolds, compared with acellular scaffolds ($P < 0.0001$), with similarly low numbers of caspase-3-positive cells in all groups ($P = 0.5483$), consistent with increased proliferation in the scaffolds containing BMSC or ADSC. Lastly, we found an increase in the numbers of VEGF-A-positive cells in wounds treated with ADSC or BMSC (Fig. 3, *B* and *D*). These results show that ADSC and BMSC promote similar types of cell infiltration, proliferation, and VEGF-A synthesis, findings consistent with our previous data (2).

Since Notch signaling has been implicated in angiogenesis (18) as well as keratinocyte specification (26), we determined whether there was any difference between BMSC- and ADSC-treated wounds in their expression of several members of the Notch signaling pathway. The expression of Notch ligands DLL-1 and CBF-1, the Notch receptor notch-1, and the Notch pathway target gene *HES-1* from the surrounding wound tissues was increased to the same degree in wounds treated with scaffolds containing BMSC or ADSC, compared with acellular scaffolds ($P < 0.05$ for DLL-1 expression; $P < 0.001$ for CBF-1, Notch-1 and *HES-1* expression) (Fig. 4, *A* and *B*). These results were confirmed using immunofluorescence, which also showed increased expression of DLL-1 and CBF-1 (Fig. 4, *C* and *D*), as well as *HES-1* and Notch-1 (Fig. 4, *E* and *F*), in both BMSC as well as ADSC compared with acellular scaffolds ($P < 0.0001$, *day 7*). There was no significant difference between BMSC and ADSC. These results demonstrate that delivery of murine ADSC upregulates the Notch signaling pathway to a similar degree as does delivery of BMSC in vivo.

Human diabetic and nondiabetic ADSC show similar morphology in vitro. Since murine ADSC are capable of improving wound healing in a diabetic mouse wound model (Figs. 2–4), they may have translational potential to human patients. Since diabetic patients may have cells with reduced healing potential compared with cells derived from nondiabetic patients, we next assessed whether human diabetic and nondiabetic ADSC show similar wound healing potential. Human ADSC derived from both nondiabetic and diabetic donors showed similar morphology in vitro (Fig. 5*A*); the expression of surface markers was consistent with mesenchymal stem cell identity in both cell

Fig. 5. Human nondiabetic and diabetic adipose tissue-derived stem cells (ADSC) show similar morphology in vitro. *A*: human ADSC show similar spindle-shaped morphology in vitro (×200, scale bar = 50 μm, in G_1, *day 3*). *Left*, nondiabetic donor source. *Right*, diabetic donor source. *B*: FACS analysis confirms identity of human ADSC with positive expression of CD105, and CD44 and lack of expression of CD45, CD34, and HLA-DR. *C*: VEGF-A expression of ADSC in the collagen scaffold at 0 h, 24 h, and 72 h. *Left* 3 panels, immunohistochemistry; *right* 3 panels, immunofluorescence (×400, scale bar = 50 μm). *D*: quantification of percentage of VEGF-A positive cells in nondiabetic and diabetic ADSC over time (*$P < 0.05$, **$P < 0.01$, ***$P < 0.001$, $n = 3$ for each group). *E*: VEGF expression via ELISA assay in diabetic and nondiabetic cells ($P > 0.05$, $n = 3$ per group). *F*: Western blot showing VEGF-A expression in nondiabetic and diabetic human ADSC and quantification of VEGF expression of human ADSC; $P = 0.668$.

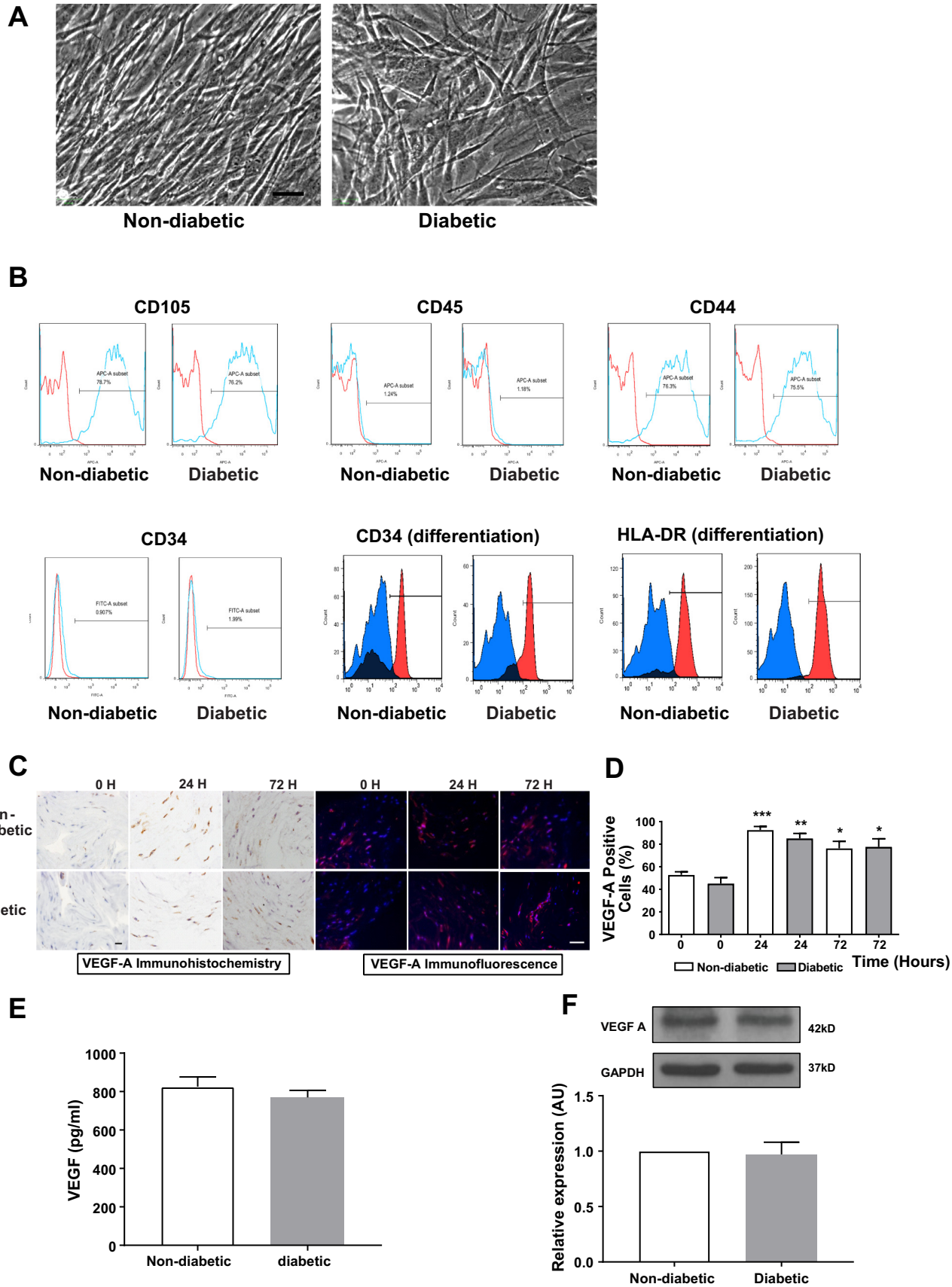

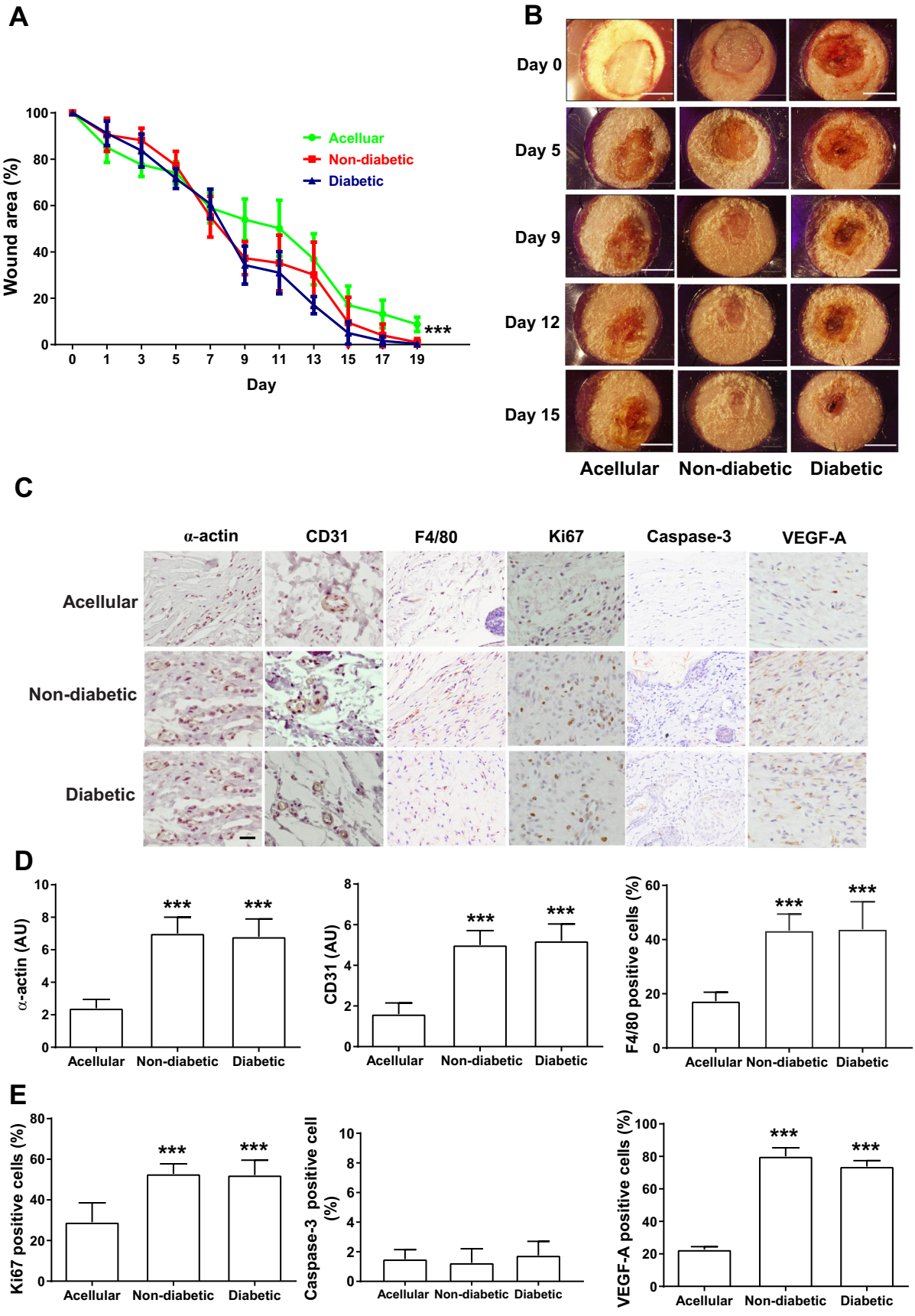

lines (Fig. 5*B*). We used CD34 and HLA-DR surface markers to show the different phenotype of undifferentiated versus differentiated cells. Both diabetic and nondiabetic cells showed an increase of CD34 surface markers from 0.13% to 75.12% in nondiabetic and from 0.21% to 71.90% in diabetic cells once differentiated; HLA-DR also increased similarly from 0.07% to 91.65% and from 0.02% to 95.71% in nondiabetic and diabetic cells, respectively (Fig. 5*B*). VEGF-A protein expression was detectable at baseline, increased by 24 h in the collagen scaffold, and was maintained by 72 h in vitro. There was no difference in number of VEGF-A-positive cells (Fig. 5, *C* and *D*), as well as VEGF protein expression between nondiabetic and diabetic ADSC by ELISA and Western blot analysis (Fig. 5, *E* and *F*).

Similar wound healing with nondiabetic and diabetic human ADSC in vivo. Collagen scaffolds containing human ADSC derived from either nondiabetic or diabetic patients were placed on splinted wounds in nude mice. Scaffolds containing human ADSC showed improved wound healing compared with acellular scaffolds ($P = 0.01$), without any difference between nondiabetic and diabetic ADSC ($P = 0.822$, post hoc; Fig. 6, *A* and *B*). There was an increased number of α-actin-positive cells in the wounds treated with human ADSC, compared with acellular scaffolds ($P = 0.0002$, post hoc), with similar number of α-actin-positive cells between diabetic and nondiabetic ADSC ($P = 0.754$, post hoc) (Fig. 6, *C* and *D*). Similarly, there were more CD31-positive cells and VEGF-A-positive cells in wounds treated with healthy ADSC, compared with acellular scaffolds, with similar numbers of positive cells in wounds treated with nondiabetic or diabetic ADSC ($P = 0.841$ and 0.293, respectively, post hoc) (Fig. 6, *C*, *D*, *E*). Lastly, there were more Ki67-positive cells in human ADSC-containing scaffolds, compared with acellular scaffolds ($P < 0.001$), with similarly low numbers of caspase-3-positive cells in all groups (Fig. 6*C*), consistent with increased proliferation in the scaffolds containing diabetic and healthy ADSC. These results suggest that delivery of human diabetic ADSC enhances wound healing similarly to nondiabetic ADSC.

DISCUSSION

Based on our previous promising result that delivery of BMSC in a biomimetic-collagen scaffold accelerates wound healing in a diabetic mouse splinted back wound model, the present study compared the therapeutic potential of ADSC, a cell type with better potential for translational studies, with that of previously studied BMSC. We found that murine ADSC delivered in a biomimetic-collagen scaffold enhance diabetic wound healing with similar therapeutic effect as BMSC. Further, human diabetic and nondiabetic ADSC are morphologically and functionally similar, with diabetic cells having comparable wound healing potential to healthy ADSC. This finding is of importance for the treatment of DFU, since these data suggest that a diabetic patient's own cells may have the same therapeutic potential as those from healthy controls, allowing for isogenic cell transfer.

ADSC are a more attractive cell type as compared with BMSC because they require less invasive aspiration methods, are a more abundant source, and are very stable under cell culture conditions with a normal haploid karyotype after 100 duplications (11). There are 10- to 1,000-fold more stromal/stem cells per unit volume of tissue as compared with BMSC (13). Previous studies have reported that collagen scaffolds enhanced the survival, migration, and differentiation of the stem cells transplanted into target tissue (10, 25, 28). Our study demonstrated MSC survival beyond 5 days after implantation, and cell survival and migration of ADSC or BMSC within the scaffolds were similar. Sheng et al. (27) found transplanted ADSC were detectable in subcutaneous and vascular vessels for up to 4 wk.

Our study indicates that ADSC delivered in a biomimetic-collagen scaffold accelerates diabetic wound healing with similar therapeutic effect as BMSC. This finding carries great clinical implications for the translation of this treatment to human trials. Consistent with published studies, local administration of ADSC in a matrix scaffold could effectively accelerate wound healing by promoting neovascularization and reepithelialization (24). We found similarly higher levels of VEGF expression in wounds treated with both BMSC and ADSC, compared with the acellular group. We also found increased CD31 density in the wound beds of MSC-treated (ADSC or BMSC) groups, compared with the acellular control group, suggesting that delivery of ADSC or BMSC promotes angiogenesis. Lastly, the muscular layer in wounds treated with stem cells was thicker, likely as a result of paracrine cell signaling and chemoattraction of host cells to the wound.

Inflammatory cells play a key role in all three phases of wound healing via wound sterilization and phagocytosis, growth factor release to promote chemotaxis, granulation tissue formation, as well as cell activation and proliferation. In particular, macrophages are essential to wound healing. Different macrophage phenotypes predominate in the wound bed during various parts of the wound healing cycle, and it has been hypothesized that retention of the proinflammatory macrophage phenotype leads to chronic wounds (19). We have previously demonstrated increased wound macrophage concentrations after delivery of mesenchymal stem cells; future studies are needed to examine the phenotype and role of infiltrating macrophages (2).

We also demonstrated that in vivo delivery of murine ADSC in a scaffold gel upregulates Notch signaling to the same extent that BMSC does. Our observation is consistent with previous literature that has shown epidermal stem cells and MSC accelerate diabetic wound healing via the Notch signaling pathway (6, 30). Pedrosa et al. (25) reported that overexpression of the Notch ligand Jag1 in endothelial cells increased vessel density, maturation, and perfusion, thus accelerating wound healing. Our results suggest that treatment of diabetic wounds may occur via upregulation of Notch signaling, resulting in increased angiogenesis.

Fig. 6. Similar wound healing with nondiabetic and diabetic human adipose tissue-derived stem cells (ADSC) in vivo. *A*: line graph shows wound size over time ($P = 0.0003$, $n = 3$ for each group). *B*: representative images of wounds at *days 0*, *5*, *9*, *12*, and *15*. *C*: representative images of immunohistochemistry showing expression of α-actin, CD31, F4/80, Ki67, caspase-3, and VEGF-A (×400 scale bar = 50 μm). *D*: quantification of percentage of positive cells (***$P < 0.001$, $n = 4$ for each group).

Our study also found that human diabetic ADSC in a scaffold gel have the same ability to improve diabetic nude mouse wound healing as nondiabetic ADSC. Though multiple studies have shown that human ADSC have the potential to increase angiogenesis and wound healing (4, 20), the therapeutic potential of ADSC derived from diabetic donors remains unclear (5, 32). We were able to demonstrate that diabetic cells are noninferior to healthy ones at upregulating VEGF expression and accelerating wound healing. Although they display differential gene expression, MSC from type 1 diabetic donors are phenotypically and functionally similar to healthy control MSC with regard to their immunomodulatory and migratory potential, indicating their suitability for use in autologous therapy (7, 30). Our results suggest that ADSC, even from diabetic patients, promote diabetic wound healing, opening the potential for large-scale clinical trials for diabetic patients. Further, our data suggest that isogenic cells lines, as well as those derived from other species, potentiate wound healing. We believe this to be the result of the paracrine effects of transplanted cells in the recipient wound environment, which lasts beyond the lifetime of transplanted cells (6). Therefore, wound healing is likely to be potentiated by release of key growth factors and recipient cell chemoattraction, which is independent of the cell source transplanted onto cutaneous wounds.

There are some limitations in the present study. First, standardized MSC manufacturing and quality control are limited by interbatch variation. Second, the streptozotocin model of diabetes more closely represents type 1 diabetes by inducing necrosis of β-pancreatic cells, which may have subtle but important effects on wound healing. Third, the wound model used in this study represents an acute insult, rather than a chronic diabetic wound. Despite these limitations, our study provides meaningful results that may be useful for future trials, particularly for diabetic patients.

In conclusion, taken together, the present study demonstrates that murine ADSC delivery in a biomimetic-collagen scaffold enhances diabetic wound healing to a similar degree as previously used BMSC, circumventing the need for invasive cell harvesting methods. Further, we have illustrated the noninferiority of diabetic ADSC on angiogenesis and promotion of wound healing as compared with cells from healthy controls, broadening the scope of therapeutic potential for autologous stem cell-based approaches for diabetic patients.

GRANTS

This work was supported by NIH National Heart, Lung, and Blood Institute Grant R01-HL128406 and by the U.S. Department of Veterans Affairs Biomedical Laboratory Research and Development Program, Merit Review Award I01-BX002336, an Association of VA Surgeons Resident Research Award, as well as through the resources and use of facilities at the Veterans Affairs Connecticut Healthcare System (West Haven, CT).

DISCLOSURES

No conflicts of interest, financial or otherwise, are declared by the authors.

AUTHOR CONTRIBUTIONS

J. Guo, H. Hu, J. Gorecka, Y. Gu, and A. Dardik conceived and designed research; J. Guo, H. Hu, J. Gorecka, H.B., H. He, R.A., T.I., and T.W. performed experiments; J. Guo, H. Hu, J. Gorecka, H.B., H. He, and A.D. analyzed data; J. Guo, H. Hu, J. Gorecka, Y.G., and A.D. interpreted results of experiments; J. Guo, H. Hu, J. Gorecka, H.B., Y.G., and A.D. prepared figures; J. Guo, H. Hu, J. Gorecka, and A.D. drafted manuscript; J. Guo, H. Hu, J. Gorecka, H.B., H. He, R.A., T.I., T.W., O.S., L.L., Y.G., and A.D. edited and revised manuscript; J. Guo, H. Hu, J. Gorecka, H.B., H. He, R.A., T.I., T.W., O.S., L.L., Y.G., and A.D. approved final version of manuscript.

REFERENCES

1. **Araña M, Mazo M, Aranda P, Pelacho B, Prosper F.** Adipose tissue-derived mesenchymal stem cells: isolation, expansion, and characterization. *Methods Mol Biol* 1036: 47–61, 2013. doi:10.1007/978-1-62703-511-8_4.
2. **Assi R, Foster TR, He H, Stamati K, Bai H, Huang Y, Hyder F, Rothman D, Shu C, Homer-Vanniasinkam S, Cheema U, Dardik A.** Delivery of mesenchymal stem cells in biomimetic engineered scaffolds promotes healing of diabetic ulcers. *Regen Med* 11: 245–260, 2016. doi:10.2217/rme-2015-0045.
3. **Brem H, Tomic-Canic M.** Cellular and molecular basis of wound healing in diabetes. *J Clin Invest* 117: 1219–1222, 2007. doi:10.1172/JCI32169.
4. **Cherubino M, Valdatta L, Balzaretti R, Pellegatta I, Rossi F, Protasoni M, Tedeschi A, Accolla RS, Bernardini G, Gornati R.** Human adipose-derived stem cells promote vascularization of collagen-based scaffolds transplanted into nude mice. *Regen Med* 11: 261–271, 2016. doi:10.2217/rme-2015-0010.
5. **Cianfarani F, Toietta G, Di Rocco G, Cesareo E, Zambruno G, Odorisio T.** Diabetes impairs adipose tissue-derived stem cell function and efficiency in promoting wound healing. *Wound Repair Regen* 21: 545–553, 2013. doi:10.1111/wrr.12051.
6. **Collawn S, Patel S.** Adipose-derived stem cells, their secretome, and wound healing. *J Cell Sci Ther* 5: 165, 2014. doi:10.4172/2157-7013.1000165.
7. **Davies LC, Alm JJ, Heldring N, Moll G, Gavin C, Batsis I, Qian H, Sigvardsson M, Nilsson B, Kyllonen LE, Salmela KT, Carlsson PO, Korsgren O, Le Blanc K.** Type 1 diabetes mellitus donor mesenchymal stromal cells exhibit comparable potency to healthy controls in vitro. *Stem Cells Transl Med* 5: 1485–1495, 2016. doi:10.5966/sctm.2015-0272.
8. **De Ugarte DA, Morizono K, Elbarbary A, Alfonso Z, Zuk PA, Zhu M, Dragoo JL, Ashjian P, Thomas B, Benhaim P, Chen I, Fraser J, Hedrick MH.** Comparison of multi-lineage cells from human adipose tissue and bone marrow. *Cells Tissues Organs* 174: 101–109, 2003. doi:10.1159/000071150.
9. **Dominici M, Le Blanc K, Mueller I, Slaper-Cortenbach I, Marini F, Krause D, Deans R, Keating A, Prockop D, Horwitz E.** Minimal criteria for defining multipotent mesenchymal stromal cells. The International Society for Cellular Therapy position statement. *Cytotherapy* 8: 315–317, 2006. doi:10.1080/14653240600855905.
10. **Duan H, Li X, Wang C, Hao P, Song W, Li M, Zhao W, Gao Y, Yang Z.** Functional hyaluronate collagen scaffolds induce NSCs differentiation into functional neurons in repairing the traumatic brain injury. *Acta Biomater* 45: 182–195, 2016. doi:10.1016/j.actbio.2016.08.043.
11. **Fromm-Dornieden C, Koenen P.** Adipose-derived stem cells in wound healing: recent results in vitro and in vivo. *OA Mol Cell Biol* 1: 8, 2013. doi:10.13172/2054-7331-1-1-1147.
12. **Galiano RD, Michaels Jt, Dobryansky M, Levine JP, Gurtner GC.** Quantitative and reproducible murine model of excisional wound healing. *Wound Repair Regen* 12: 485–492, 2004. doi:10.1111/j.1067-1927.2004.12404.x.
13. **Gimble JM, Katz AJ, Bunnell BA.** Adipose-derived stem cells for regenerative medicine. *Circ Res* 100: 1249–1260, 2007. doi:10.1161/01.RES.0000265074.83288.09.
14. **Gonzalez-Rey E, Gonzalez MA, Varela N, O'Valle F, Hernandez-Cortes P, Rico L, Büscher D, Delgado M.** Human adipose-derived mesenchymal stem cells reduce inflammatory and T cell responses and induce regulatory T cells in vitro in rheumatoid arthritis. *Ann Rheum Dis* 69: 241–248, 2010. doi:10.1136/ard.2008.101881.
15. **Guest JF, Fuller GW, Vowden P.** Diabetic foot ulcer management in clinical practice in the UK: costs and outcomes. *Int Wound J* 15: 43–52, 2018. doi:10.1111/iwj.12816.
16. **Guo S, Dipietro LA.** Factors affecting wound healing. *J Dent Res* 89: 219–229, 2010. doi:10.1177/0022034509359125.
17. **Hicks CW, Canner JK, Karagozlu H, Mathioudakis N, Sherman RL, Black JH III, Abularrage CJ.** The Society for Vascular Surgery Wound, Ischemia, and foot Infection (WIfI) classification system correlates with cost of care for diabetic foot ulcers treated in a multidisciplinary setting. *J Vasc Surg* 67: 1455–1462, 2018. doi:10.1016/j.jvs.2017.08.090.

18. **Kofler NM, Shawber CJ, Kangsamaksin T, Reed HO, Galatioto J, Kitajewski J.** Notch signaling in developmental and tumor angiogenesis. *Genes Cancer* 2: 1106–1116, 2011. doi:10.1177/1947601911423030.
19. **Krzyszczyk P, Schloss R, Palmer A, Berthiauma F.** The role of macrophages in acute and chronic wound healing and interventions to promote pro-wound healing phenotypes. *Front Physiol* 1: 9, 2018. doi:10.3389/fphys.2018.00419.
20. **Lee DE, Ayoub N, Agrawal DK.** Mesenchymal stem cells and cutaneous wound healing: novel methods to increase cell delivery and therapeutic efficacy. *Stem Cell Res Ther* 7: 37, 2016. doi:10.1186/s13287-016-0303-6.
21. **Mathioudakis N, Hicks CW, Canner JK, Sherman RL, Hines KF, Lum YW, Perler BA, and Abularrage CJ.** The Society for Vascular Surgery Wound, Ischemia, and foot Infection (WIfI) classification system predicts wound healing but not major amputation in patients with diabetic foot ulcers treated in a multidisciplinary setting. *J Vasc Surg* 65: 1698–1705.e1691, 2017.
22. **Menke NB, Ward KR, Witten TM, Bonchev DG, Diegelmann RF.** Impaired wound healing. *Clin Dermatol* 25: 19–25, 2007. doi:10.1016/j.clindermatol.2006.12.005.
23. **Meza-Zepeda LA, Noer A, Dahl JA, Micci F, Myklebost O, Collas P.** High-resolution analysis of genetic stability of human adipose tissue stem cells cultured to senescence. *J Cell Mol Med* 12: 553–563, 2008. doi:10.1111/j.1582-4934.2007.00146.x.
24. **Nie C, Yang D, Morris SF.** Local delivery of adipose-derived stem cells via acellular dermal matrix as a scaffold: a new promising strategy to accelerate wound healing. *Med Hypotheses* 72: 679–682, 2009. doi:10.1016/j.mehy.2008.10.033.
25. **Qi C, Yan X, Huang C, Melerzanov A, Du Y.** Biomaterials as carrier, barrier and reactor for cell-based regenerative medicine. *Protein Cell* 6: 638–653, 2015. doi:10.1007/s13238-015-0179-8.
26. **Rangarajan A, Talora C, Okuyama R, Nicolas M, Mammucari C, Oh H, Aster JC, Krishna S, Metzger D, Chambon P, Miele L, Aguet M, Radtke F, Dotto GP.** Notch signaling is a direct determinant of keratinocyte growth arrest and entry into differentiation. *EMBO J* 20: 3427–3436, 2001. doi:10.1093/emboj/20.13.3427.
27. **Sheng L, Yang M, Liang Y, Li Q.** Adipose tissue-derived stem cells (ADSCs) transplantation promotes regeneration of expanded skin using a tissue expansion model. *Wound Repair Regen* 21: 746–754, 2013. doi:10.1111/wrr.12080.
28. **Somaiah C, Kumar A, Mawrie D, Sharma A, Patil SD, Bhattacharyya J, Swaminathan R, Jaganathan BG.** Collagen promotes higher adhesion, survival and proliferation of mesenchymal stem cells. *PLoS One* 10: e0145068, 2015. doi:10.1371/journal.pone.0145068.
29. **Yang M, Sheng L, Zhang TR, Li Q.** Stem cell therapy for lower extremity diabetic ulcers: where do we stand? *BioMed Res Int* 2013: 462179, 2013. doi:10.1155/2013/462179.
30. **Yang RH, Qi SH, Shu B, Ruan SB, Lin ZP, Lin Y, Shen R, Zhang FG, Chen XD, Xie JL.** Epidermal stem cells (ESCs) accelerate diabetic wound healing via the Notch signalling pathway. *Biosci Rep* 36: e00364, 2016. doi:10.1042/BSR20160034.
31. **Zhang P, Lu J, Jing Y, Tang S, Zhu D, Bi Y.** Global epidemiology of diabetic foot ulceration: a systematic review and meta-analysis. *Ann Med* 49: 106–116, 2017. doi:10.1080/07853890.2016.1231932.
32. **Zografou A, Papadopoulos O, Tsigris C, Kavantzas N, Michalopoulos E, Chatzistamatiou T, Papassavas A, Stavropoulou-Gioka C, Dontas I, Perrea D.** Autologous transplantation of adipose-derived stem cells enhances skin graft survival and wound healing in diabetic rats. *Ann Plast Surg* 71: 225–232, 2013. doi:10.1097/SAP.0b013e31826af01a.